SIAM J. APPL. MATH.
Vol. 68, No. 4, pp. 907–924

THE FACTORIZATION METHOD FOR ELECTRICAL IMPEDANCE TOMOGRAPHY IN THE HALF-SPACE*

MARTIN HANKE† AND BIRGIT SCHAPPEL†

Abstract. We consider the inverse problem of electrical impedance tomography in a conducting half-space, given electrostatic measurements on its boundary, i.e., a hyperplane. We first provide a rigorous weak analysis of the corresponding forward problem and then develop a numerical algorithm to solve an associated inverse problem. This inverse problem consists of the reconstruction of certain inclusions within the half-space which have a different conductivity than the background. To solve the inverse problem we employ the so-called factorization method of Kirsch, which so far has only been considered for the impedance tomography problem in bounded domains. Our analysis of the forward problem makes use of a Liouville-type argument which says that a harmonic function in the entire two-dimensional plane must be a constant if some weighted L^2-norm of this function is bounded.

Key words. electrical impedance tomography, half-space problem, factorization method

AMS subject classifications. 65N21, 35R30, 35J20, 35D05, 31A05

DOI. 10.1137/06067064X

1. Introduction. Electrical impedance tomography (EIT) is a technique to recover information of the interior of a conducting object from electrostatic measurements taken on its boundary. In mathematical terms, this amounts to recovering information about the spatially varying (nonnegative) conductivity σ in the elliptic partial differential equation

$$\nabla \cdot \sigma \nabla u = 0 \qquad \text{in } B \tag{1.1}$$

from Neumann and Dirichlet boundary values of all stationary electric potentials u. This inverse boundary value problem goes back to Calderón [8] who considered (1.1) in a *bounded* domain B, provoking substantial interest in the medical imaging community.

In geoelectric applications, on the other hand, the domain B and its boundary are typically very large compared to the small fraction of its boundary where data can be measured. Therefore it makes sense to reconsider the inverse boundary value problem for (1.1) in *unbounded* domains B with *unbounded* boundary ∂B, with the half-space being the most obvious and prominent example. Another application for this model problem concerns the automatic recognition of gesture input for interactive displays, called touchless interaction, which has recently been considered by van Berkel and Lionheart [26]. Finally, in its original medical context, the half-space problem may serve as an appropriate model for certain mammography systems (cf., e.g., [2, 16, 22]) where measurements are taken on only a small portion of the patient's skin.

For the half-space B, Druskin [11] has shown that the conductivity can be reconstructed from the knowledge of the boundary data on a subdomain $\Gamma \subset \partial B$, provided that B can be subdivided into a finite set of domains with piecewise smooth boundaries and constant conductivities, respectively. In this paper we are concerned with

*Received by the editors September 25, 2006; accepted for publication (in revised form) June 19, 2007; published electronically January 30, 2008.
http://www.siam.org/journals/siap/68-4/67064.html
†Institut für Mathematik, Johannes Gutenberg-Universität Mainz, 55099 Mainz, Germany (hanke@math.uni-mainz.de, schappel@math.uni-mainz.de).

numerical algorithms to reconstruct the conductivity σ or partial information about it. In general, reconstruction methods can be divided into iterative and direct methods (we refer to Borcea [4, 5] for a relatively recent survey with the focus on bounded domains), but concerning unbounded domains B we are aware only of previous algorithms based on linearization with or without an outer iteration; cf. Lukaschewitsch, Maass, and Pidcock [20, 21], Mueller, Isaacson, and Newell [22], and the references therein. Iterative methods require the repeated solution of forward problems in each iteration, i.e., differential equations, which tends to be extremely time-consuming. We therefore present a noniterative reconstruction algorithm which can be used to detect abrupt local deviations of the conductivity from a homogenous background conductivity.

Our method is a variation of the so-called *factorization method* which goes back to an idea of Kirsch [18] in the context of inverse scattering and has been applied successfully to the impedance tomography problem by Brühl [6, 7]. In these and subsequent papers all authors have formulated the problem in either bounded domains or all of $\mathbb{R}^n$, thus avoiding the difficulties that arise with domains with unbounded boundaries. Here we employ a general framework developed by Gebauer [12] to adapt this method to the case of the half-space

$$B = \mathbb{R}^n_+ = \{x \in \mathbb{R}^n : x \cdot e_n > 0\},$$

with $e_n \in \mathbb{R}^n$ a given unit vector, the inner normal vector on ∂B. Most results will be presented for the case $n = 3$, but at the end of this paper we will give a short summary of the two-dimensional case.

For our approach we assume a constant background conductivity $\sigma_{\mathbf{1}} = \mathbf{1}$, where $\mathbf{1}$ is the function identically 1, and consider conductivities of the form

$$\sigma(x) = \begin{cases} \kappa(x), & x \in \overline{\Omega}, \\ 1, & x \in \mathbb{R}^3_+ \setminus \overline{\Omega}, \end{cases} \tag{1.2}$$

where $\Omega \subset B$ is a finite collection of separated and bounded domains with sufficiently smooth boundary $\Sigma = \partial\Omega$, and for which $\mathbb{R}^n_+ \setminus \overline{\Omega}$ is connected. Below we will denote by ν the normal of Σ pointing into Ω.

The positive conductivity $\kappa \in L^\infty(\Omega)$ is assumed to be significantly higher or lower than the background conductivity; i.e., there exists $\varepsilon > 0$ such that

$$\kappa(x) \geq 1 + \varepsilon \quad \text{or} \quad \varepsilon \leq \kappa(x) \leq 1 - \varepsilon \qquad \text{for } x \in \overline{\Omega}. \tag{1.3}$$

By means of the factorization method we provide an explicit characterization of the inclusions Ω in terms of the (local) Neumann–Dirichlet operator Λ_σ which maps Neumann boundary values of a potential u in (1.1) to its Dirichlet boundary values.

We should mention that in principle it should be possible to relax the assumption that the background conductivity is constant. However, the numerical implementation of our method will then become much more difficult, as the algorithm requires the availability of the associated Neumann function.

The paper is organized as follows: We first introduce appropriate function spaces to deal with the forward problem (1.1) in the half-space $B = \mathbb{R}^3_+$, and then clarify our notion of weak solutions of (1.1) and their existence. The inverse problem and some preliminary statements will be specified in section 3. Then, in sections 4 and 5 we prove the characterization of inclusions from the knowledge of Λ_σ. In section 6 we comment on our numerical algorithm and present some reconstructions based

on simulated data. To conclude, we briefly comment in section 7 on the necessary modifications of our theory in two space dimensions.

In an appendix we establish a Liouville-type result for harmonic functions in the plane which we use to show that certain apparently different function spaces over $\mathbb{R}^3_+$ which have been introduced in the literature, and which are relevant for our problem, are essentially the same.

2. Function spaces and weak solutions of the forward problem. The forward problem associated with impedance tomography in the half-space is the Neumann problem

$$\nabla \cdot \sigma \nabla u = 0 \quad \text{in } \mathbb{R}^3_+, \qquad -\sigma \frac{\partial u}{\partial e_3} = f \quad \text{on } \mathbb{R}^2, \tag{2.1}$$

together with an appropriate growth condition near infinity. Problem (2.1) represents the physical process of injecting a current f into the upper half-space $B = \mathbb{R}^3_+$ from its boundary. In this section the conductivity σ is assumed to be bounded and strictly positive in $\mathbb{R}^3_+$. In (2.1) and in the remainder of this paper, we always identify the boundary of $\mathbb{R}^3_+$ with $\mathbb{R}^2$, with straightforward abuse of notation.

Care has to be taken concerning the correct behavior of $u(x)$ for $|x| \to \infty$ which is reflected by the choice of appropriate function spaces for the solution u. For example, physically relevant solutions of problem (2.1)—like the fundamental solution of the Laplace equation—need not belong to the Sobolev space $H^1(\mathbb{R}^3_+)$.

Example 2.1 (see [21]). For $\sigma = \mathbf{1}$ and $f(y) = (1 + |y|^2)^{-3/2}$, a solution of (2.1) is given by $u(x) = |x + e_3|^{-1}$. It is easy to see that u does not belong to $L^2(\mathbb{R}^3_+)$; however, the gradient of u is square integrable on $\mathbb{R}^3_+$.

To construct a suitable function space we recall the following familiar definitions and notation. For a (possibly unbounded) domain $G \subset \mathbb{R}^3$ we take $C_0^\infty(G)$ to be the set of all functions $u \in C^\infty(G)$ with compact support $\operatorname{supp} u$, and let

$$C_0^\infty(\overline{G}) = \{u|_G : u \in C_0^\infty(\mathbb{R}^3)\}.$$

Furthermore, $\mathcal{D}'(G)$ is the set of distributions, i.e., the continuous linear functionals on $C_0^\infty(G)$.

In view of the physical setting (and in accordance with Example 2.1) it appears appropriate to restrict our attention to solutions of (2.1) with finite energy, which means that the H^1-seminorm of u is finite. Note that this seminorm is actually a norm on $C_0^\infty(\overline{\mathbb{R}^3_+})$ because constant functions do not belong to this set. We write $H(\mathbb{R}^3_+)$ for the closure of $C_0^\infty(\overline{\mathbb{R}^3_+})$ with respect to this norm, denoted subsequently by $\|\cdot\|_{H(\mathbb{R}^3_+)}$. According to Boulmezaoud [3], this space coincides with the weighted Sobolev space

$$\{u \in \mathcal{D}'(\mathbb{R}^3_+) : (1 + |x|^2)^{-1/2} u \in L^2(\mathbb{R}^3_+),\ \nabla u \in L^2(\mathbb{R}^3_+)^3\}. \tag{2.2}$$

Obviously, we have $H(\mathbb{R}^3_+) \subset H^1_{\mathrm{loc}}(\mathbb{R}^3_+)$, and for every bounded domain $G \subset \mathbb{R}^3_+$ the restriction operator $u \mapsto u|_G$ is continuous as a mapping from $H(\mathbb{R}^3_+) \to H^1(G)$. We point out here that for the two-dimensional case the analogous completion of $C_0^\infty(\overline{\mathbb{R}^2_+})$ with respect to the H^1-seminorm does not yield a space of distributions (cf. Deny and Lions [10]), and we refer to section 7 for the modifications which are necessary in two space dimensions.

It has been shown by Janßen [17] that every function $u \in H(\mathbb{R}^3_+)$ has a trace in

$$L^{2,1}(\mathbb{R}^2) = \{g : (1 + |y|^2)^{-1/2} g \in L^2(\mathbb{R}^2)\},$$

and that the trace operator is continuous with respect to the norm

$$\|g\|^2_{L^{2,1}(\mathbb{R}^2)} = \int_{\mathbb{R}^2} (1+|y|^2)^{-1} g^2(y)\,\mathrm{d}y$$

of $L^{2,1}(\mathbb{R}^2)$. Note that the dual space of $L^{2,1}(\mathbb{R}^2)$ can be identified with

$$L^{2,-1}(\mathbb{R}^2) = \{f : (1+|y|^2)^{1/2} f \in L^2(\mathbb{R}^2)\}$$

using $L^2(\mathbb{R}^2)$ as a pivot space in the Gelfand triple. The associated norm of $L^{2,-1}(\mathbb{R}^2)$ is denoted by $\|\cdot\|_{L^{2,-1}(\mathbb{R}^2)}$, the dual pairing between $L^{2,-1}(\mathbb{R}^2)$ and $L^{2,1}(\mathbb{R}^2)$ by

$$\langle f, g\rangle_{\mathbb{R}^2} = \int_{\mathbb{R}^2} f(y) g(y)\,\mathrm{d}y.$$

Now we return to the Neumann problem (2.1) for $u \in H(\mathbb{R}^3_+)$. The corresponding weak formulation follows in the usual way by making use of Green's formula for $u, v \in H(\mathbb{R}^3_+)$ established in [3]: Find $u \in H(\mathbb{R}^3_+)$ such that

$$\int_{\mathbb{R}^3_+} \sigma \nabla u \cdot \nabla v\,\mathrm{d}x = \int_{\mathbb{R}^2} f v\,\mathrm{d}y \qquad \text{for all } v \in H(\mathbb{R}^3_+). \tag{2.3}$$

Problem (2.3) is well defined for every $f \in L^{2,-1}(\mathbb{R}^2)$, and a standard application of the Lax–Milgram lemma establishes existence of a unique solution $u \in H(\mathbb{R}^3_+)$ of (2.3) with

$$\|u\|_H(\mathbb{R}^3_+) \le c\|f\|_{L^{2,-1}(\mathbb{R}^2)} \tag{2.4}$$

for some constant $c > 0$ depending only on the conductivity σ. We call u the weak solution of problem (2.1).

Example 2.2. If $\sigma = \mathbf{1}$, i.e., if we consider the Laplace equation, then

$$u(x) = \frac{1}{2\pi} \int_{\mathbb{R}^2} \frac{f(y)}{|x-y|}\,\mathrm{d}y, \qquad x \in \mathbb{R}^3_+, \tag{2.5}$$

is the physically relevant classical solution of problem (2.1) provided that f is continuous and that there exists a positive and monotonic function $\varepsilon \in L^1(\mathbb{R}^+)$ such that $|f(y)| \le \varepsilon(|y|)$; see, e.g., Dautray and Lions [9, Chapter II]. In particular, for $f(y) = (1+|y|^2)^{-3/2}$ this yields the function u of Example 2.1. For arbitrary $f \in L^{2,-1}(\mathbb{R}^2)$ the integral representation (2.5) defines the weak solution $u \in H(\mathbb{R}^3_+)$, as is most easily seen by using the Kelvin transformation; see [25] for further details.

Remark 2.3. In principle one can alternatively start with $C^\infty(\mathbb{R}^3_+)$ instead of $C_0^\infty(\overline{\mathbb{R}^3_+})$ and consider for some $\alpha \ge 0$ the completion $W^1_\alpha(\mathbb{R}^3_+)$ of

$$\{u \in C^\infty(\mathbb{R}^3_+) : (1+|x|^2)^{-1/2-\alpha/2} u \in L^2(\mathbb{R}^3_+),\ \nabla u \in L^2(\mathbb{R}^3_+)^3\}$$

with respect to the norm

$$\|u\|^2_{W^1_\alpha(\mathbb{R}^3_+)} = \int_{\mathbb{R}^3_+} (1+|x|^2)^{-1-\alpha} u^2(x)\,\mathrm{d}x + \int_{\mathbb{R}^3_+} |\nabla u(x)|^2\,\mathrm{d}x; \tag{2.6}$$

cf. [17] and [21]. With an argument due to Hanouzet [15, Théorème I.1] it can be shown that for $\alpha = 0$ this space coincides with $H(\mathbb{R}^3_+)$.

Because of a Poincaré-type inequality established in [21, Theorem 2.10], the spaces $W^1_\alpha(\mathbb{R}^3_+)$ with $\alpha > 1/2$ are all the same and contain $H(\mathbb{R}^3_+)$ as a closed subspace; we denote this space by $H_{1/2+}(\mathbb{R}^3_+)$ and remark that $H(\mathbb{R}^3_+)$ is a proper subspace of $H_{1/2+}(\mathbb{R}^3_+)$ because the latter includes the constants. As we will prove in the appendix, we have, in fact,

$$H_{1/2+}(\mathbb{R}^3_+) = H(\mathbb{R}^3_+) \oplus \operatorname{span}\{\mathbf{1}\}; \tag{2.7}$$

i.e., $H_{1/2+}(\mathbb{R}^3_+)$ is made up only from $H(\mathbb{R}^3_+)$ and the constants.

Yet another variant, considered in [21], is to start with C^∞-functions in $\mathbb{R}^3_+$ which are vanishing for $|x| \to \infty$. The completion of this space with respect to the norm (2.6) always yields the space $H(\mathbb{R}^3_+)$ no matter what value of $\alpha \geq 0$ is used [25, Appendix A].

Thus, both of the aforementioned variants lead essentially to the same notion of a weak solution of problem (2.1), for the constants always belong to the null space of the differential operator under consideration.

3. Basic properties of the inverse problem. Now we are going to specify somewhat further the impedance tomography problem we consider in this paper. We shall assume throughout that the conductivity σ has the form given in (1.2), (1.3) and recall that, by virtue of (2.4), we have a well-defined bounded linear operator from $L^{2,-1}(\mathbb{R}^2)$ into $H(\mathbb{R}^3_+)$ which maps a given boundary current $f \in L^{2,-1}(\mathbb{R}^2)$ onto the induced potential $u_\sigma \in H(\mathbb{R}^3_+)$. By passing on to the trace of u_σ on $\mathbb{R}^2$ we obtain the *Neumann–Dirichlet operator*

$$\Lambda^g_\sigma : L^{2,-1}(\mathbb{R}^2) \to L^{2,1}(\mathbb{R}^2), \qquad f \mapsto u_\sigma|_{\mathbb{R}^2}.$$

Here, the superscript g stands for *global*, because for practical purposes it is often sufficient to restrict the attention to currents f supported on some bounded subset $\Gamma \subset \mathbb{R}^2$, and also to confine oneself to taking measurements of u_σ only on Γ. This gives rise to the so-called *local Neumann–Dirichlet operator*

$$\Lambda^\ell_\sigma : L^2(\Gamma) \to L^2(\Gamma), \qquad f|_\Gamma \mapsto u_\sigma|_\Gamma.$$

It is easy to check that there holds

$$\Lambda^\ell_\sigma = P \Lambda^g_\sigma P', \tag{3.1}$$

where P is the projection

$$P : L^{2,1}(\mathbb{R}^2) \to L^2(\Gamma), \qquad g \mapsto g|_\Gamma,$$

and

$$P' : L^2(\Gamma) \to L^{2,-1}(\mathbb{R}^2), \qquad f \mapsto \begin{cases} f(y), & y \in \Gamma, \\ 0, & y \in \mathbb{R}^2 \setminus \Gamma, \end{cases}$$

is the dual operator of P.

Our inverse problem is now the following:

> *Let the conductivity σ be of the form (1.2) with κ as in (1.3), and let Λ^g_σ—or Λ^ℓ_σ for some bounded and relatively open subset $\Gamma \subset \mathbb{R}^2$, respectively—be given. How can we reconstruct the support of κ, i.e., the discontinuities of σ?*

Before we proceed to derive a constructive answer to this question, we list some elementary properties of the operators Λ_σ^g and Λ_σ^ℓ.

LEMMA 3.1.

(i) $\Lambda_\sigma^\ell : L^2(\Gamma) \to L^2(\Gamma)$ *is compact, self-adjoint, and positive.*

(ii) *Let* $f \in L^{2,-1}(\mathbb{R}^2)$, *and let* $\sigma_1, \sigma_2 \in L^\infty(\mathbb{R}^3_+)$ *with* $\sigma_1, \sigma_2 \geq \varepsilon$ *almost everywhere in* $\mathbb{R}^3_+$. *Then, if* $\sigma_1 \leq \sigma_2$, *we have*

$$\langle f, \Lambda_{\sigma_1}^g f\rangle_{\mathbb{R}^2} \geq \langle f, \Lambda_{\sigma_2}^g f\rangle_{\mathbb{R}^2}.$$

Proof. Consider some bounded domain $G \subset \mathbb{R}^3_+$ with $\Gamma \subset \partial G$. Then, as mentioned before, the operator which restricts $u \in H(\mathbb{R}^3_+)$ to $u|_G \in H^1(G)$ is bounded, and the trace operator from $H^1(G)$ to $L^2(\Gamma)$ is compact. Hence, Λ_σ^ℓ is compact.

Let $0 \neq f$, $\tilde f \in L^2(\Gamma)$, and $u_\sigma, \tilde u_\sigma \in H(\mathbb{R}^3_+)$ be the solutions of (2.3) with $f' = P'f$ and $\tilde f' = P'\tilde f$, respectively. Then by virtue of (3.1) we have

$$\langle f, \Lambda_\sigma^\ell \tilde f\rangle_{L^2(\Gamma)} = \langle f', \Lambda_\sigma^g \tilde f'\rangle_{\mathbb{R}^2} = \int_{\mathbb{R}^3_+} \sigma \nabla u_\sigma \cdot \nabla \tilde u_\sigma \, \mathrm{d}x = \langle \tilde f, \Lambda_\sigma^\ell f\rangle_{L^2(\Gamma)}.$$

Thus Λ_σ^ℓ is self-adjoint. With $f = \tilde f$ we obtain, using (1.3), that

$$\langle f, \Lambda_\sigma^\ell f\rangle_{L^2(\Gamma)} = \int_{\mathbb{R}^3_+} \sigma |\nabla u_\sigma|^2 \, \mathrm{d}x \geq \varepsilon \int_{\mathbb{R}^3_+} |\nabla u_\sigma|^2 \, \mathrm{d}x = \varepsilon \|u_\sigma\|^2_{H(\mathbb{R}^3_+)},$$

and hence, Λ_σ^ℓ is positive.

Now, let $f \in L^{2,-1}(\mathbb{R}^2)$ be given, and let $u_{\sigma_1}, u_{\sigma_2} \in H(\mathbb{R}^3_+)$ be the weak solutions of (2.1) for the two conductivities σ_1 and σ_2, respectively. From (2.3) it follows that u_{σ_1} is the unique minimizer in $H(\mathbb{R}^3_+)$ of the quadratic energy functional

$$\frac{1}{2} \int_{\mathbb{R}^3_+} \sigma_1 |\nabla u|^2 \, dx - \langle f, u\rangle_{\mathbb{R}^2}$$

with minimum value $-\frac{1}{2}\langle f, u_{\sigma_1}\rangle_{\mathbb{R}^2}$. Therefore

$$\begin{aligned} -\frac{1}{2}\langle f, \Lambda_{\sigma_1}^g f\rangle_{\mathbb{R}^2} &= \frac{1}{2} \int_{\mathbb{R}^3_+} \sigma_1 |\nabla u_{\sigma_1}|^2 \, \mathrm{d}x - \langle f, u_{\sigma_1}\rangle_{\mathbb{R}^2} \\ &\leq \frac{1}{2} \int_{\mathbb{R}^3_+} \sigma_1 |\nabla u_{\sigma_2}|^2 \, \mathrm{d}x - \langle f, u_{\sigma_2}\rangle_{\mathbb{R}^2} \\ &\leq \frac{1}{2} \int_{\mathbb{R}^3_+} \sigma_2 |\nabla u_{\sigma_2}|^2 \, \mathrm{d}x - \langle f, u_{\sigma_2}\rangle_{\mathbb{R}^2} = -\frac{1}{2}\langle f, \Lambda_{\sigma_2}^g f\rangle_{\mathbb{R}^2}, \end{aligned} \tag{3.2}$$

which was to be shown. ∎

Our approach to the solution of the inverse problem is based on a comparison of the measured Neumann–Dirichlet operator Λ_σ^g or Λ_σ^ℓ with the reference operator $\Lambda_{\mathbf{1}}^g$ or $\Lambda_{\mathbf{1}}^\ell$, respectively, corresponding to the homogeneous background with conductivity $\mathbf{1}$. From Lemma 3.1 we immediately conclude the following.

COROLLARY 3.2. *Under the assumptions* (1.2), (1.3), $\Lambda_\sigma^g - \Lambda_{\mathbf{1}}^g$ *as well as* $\Lambda_\sigma^\ell - \Lambda_{\mathbf{1}}^\ell$ *are self-adjoint and positive (resp., negative) if* $\kappa \leq 1 - \varepsilon$ *(resp.,* $\kappa \geq 1 + \varepsilon$*).*

Proof. An adaptation of the proof of Lemma 3.1(i) establishes that Λ_σ^g and $\Lambda_{\mathbf{1}}^g$ are self-adjoint. For the remainder of the proof we consider only the case where $\kappa \leq 1 - \varepsilon$

for some $\varepsilon > 0$; the other case is treated similarly. For this situation we obtain from Lemma 3.1 that

$$\langle f, (\Lambda_\sigma^g - \Lambda_{\mathbf{1}}^g) f \rangle_{\mathbb{R}^2} = \langle f, \Lambda_\sigma^g f \rangle_{\mathbb{R}^2} - \langle f, \Lambda_{\mathbf{1}}^g f \rangle_{\mathbb{R}^2} \geq 0 \tag{3.3}$$

for every $f \in L^{2,-1}(\mathbb{R}^2)$; moreover, strict inequality holds in (3.2), and thus in (3.3), if the two potentials u_σ and $u_{\mathbf{1}}$ occurring in the proof of Lemma 3.1 are different.

Thus, assuming equality in (3.3) for some $f \in L^{2,-1}(\mathbb{R}^2)$, we can conclude that

$$0 = \langle f, \Lambda_\sigma^g f \rangle_{\mathbb{R}^2} - \langle f, \Lambda_{\mathbf{1}}^g f \rangle_{\mathbb{R}^2} = \int_\Omega (\kappa - 1) |\nabla u_{\mathbf{1}}|^2 \, \mathrm{d}x,$$

and hence, $u_{\mathbf{1}}$ is constant in Ω. Since $u_{\mathbf{1}}$ is harmonic in $\mathbb{R}^3_+$, this implies that it is constant in the entire half-space. It follows that $f = 0$, which proves that $\Lambda_\sigma^g - \Lambda_{\mathbf{1}}^g$ is positive.

For the local Neumann–Dirichlet operators we consider $f \in L^2(\Gamma)$, and set $f' = P'f$. By virtue of (3.1) we obtain

$$\langle f, (\Lambda_\sigma^\ell - \Lambda_{\mathbf{1}}^\ell) f \rangle_{L^2(\Gamma)} = \langle f', (\Lambda_\sigma^g - \Lambda_{\mathbf{1}}^g) f' \rangle_{\mathbb{R}^2},$$

where the latter is positive according to the first part of this proof, unless $f = 0$. Therefore $\Lambda_\sigma^\ell - \Lambda_{\mathbf{1}}^\ell$ is also a positive operator. ∎

4. The framework for the factorization method. In what follows our notation will no longer make explicit whether we are talking about local or global measurements; i.e., we write Λ_σ for either Λ_σ^g or Λ_σ^ℓ. Furthermore, we denote by $T = \mathbb{R}^2$ or $T = \Gamma$ the domain, on which measurements shall be taken. In accordance with this notation, we let $H(T)$ be either $L^{2,1}(\mathbb{R}^2)$ or $L^2(\Gamma)$, respectively.

To simplify the presentation we will assume throughout that Ω consists of only one connected component. Our theory extends to the general case, and whenever necessary we will point out the appropriate modifications for this more general situation (see also [24]).

We want to apply the general framework of Gebauer and therefore adopt his notation from [12] in what follows. We first introduce, similar to $H(B) = H(\mathbb{R}^3_+)$, a function space $H(Q)$ on $Q = B \setminus \overline{\Omega}$ by closing $C_0^\infty(\overline{Q})$ with respect to the H^1-seminorm, which will be denoted by $\|\cdot\|_{H(Q)}$. The space $H(Q)$ has properties similar to those of $H(B)$. In particular, there is a continuous trace operator $\gamma_{Q\to T}$ from $H(Q)$ to $H(T)$, and $H(Q)$ is continuously embedded in $H^1(G \setminus \overline{\Omega})$ for any bounded neighborhood $G \subset \mathbb{R}^3_+$ of Ω. For $u \in H(Q)$ we can thus define a normalized trace operator

$$\gamma_{Q\to\Sigma} v = v - \frac{\mathbf{1}}{|\Sigma|} \int_\Sigma v \, \mathrm{d}o, \qquad v \in H(Q). \tag{4.1}$$

Here, $|\Sigma|$ is the volume of the surface Σ, and $\gamma_{Q\to\Sigma}$ is a bounded and surjective operator from $H(Q)$ onto

$$H(\Sigma) = \left\{ v \in H^{1/2}(\Sigma) : \int_\Sigma v \, \mathrm{d}o = 0 \right\}.$$

In accordance with $H(\Sigma)$ we also introduce the function space

$$H(\Omega) = \left\{ w \in H^1(\Omega) : \int_\Sigma w \, \mathrm{d}o = 0 \right\},$$

which, again, can be equipped with the H^1-seminorm, so that the usual trace operator $\gamma_{\Omega\to\Sigma}$ maps $H(\Omega)$ continuously onto $H(\Sigma)$. We mention that the need for a Poincaré-type inequality is the reason to enforce vanishing means over Σ for elements from $H(\Omega)$.[1]

The framework of Gebauer also requires a linkage between the spaces $H(B)$, $H(Q)$, and $H(\Omega)$. In particular, we need to define "restriction operators" $E_Q : H(B) \to H(Q)$ and $E_\Omega : H(B) \to H(\Omega)$. In fact, we can take the natural restriction for E_Q, i.e., $E_Q u = u|_Q$, but we need to be more careful in the definition of E_Ω: Similarly to (4.1), we let

$$E_\Omega u = u|_\Omega - \frac{\mathbf{1}}{|\Sigma|}\int_\Sigma u \,\mathrm{d}o, \qquad u \in H(B), \tag{4.2}$$

such that the compatibility condition $\gamma_{Q\to\Sigma} E_Q = \gamma_{\Omega\to\Sigma} E_\Omega$ holds true.

Classical extension operators

$$\gamma^-_{Q\to\Sigma} : H(\Sigma) \to H(Q) \qquad \text{and} \qquad \gamma^-_{\Omega\to\Sigma} : H(\Sigma) \to H(\Omega)$$

yield continuous right inverses of the two "trace operators." Note that $\gamma_{\Omega\to\Sigma}$ has a continuous extension to the classical trace operator $\hat\gamma_{\Omega\to\Sigma} : H^1(\Omega) \to H^{1/2}(\Sigma)$, and likewise, $\gamma^-_{\Omega\to\Sigma}$ has a continuous extension to a right inverse $\hat\gamma^-_{\Omega\to\Sigma} : H^{1/2}(\Sigma) \to H^1(\Omega)$ of $\hat\gamma_{\Omega\to\Sigma}$ by setting $\hat\gamma^-_{\Omega\to\Sigma}\mathbf{1} = \mathbf{1}$.

In addition we need to construct continuous right inverses E^-_Q and E^-_Ω of E_Q and E_Ω, respectively. To this end we set

$$E^-_\Omega w = \begin{cases} w & \text{on } \Omega, \\ \gamma^-_{Q\to\Sigma}\gamma_{\Omega\to\Sigma} w & \text{on } Q, \end{cases} \qquad \text{and} \qquad E^-_Q v = \begin{cases} \hat\gamma^-_{\Omega\to\Sigma} v|_\Sigma & \text{on } \Omega, \\ v & \text{on } Q. \end{cases}$$

It follows, e.g., from Renardy and Rogers [23, Lemma 6.85], that these piecewise defined functions belong to $H^1_{\mathrm{loc}}(\mathbb{R}^3_+)$, and that E^-_Ω and E^-_Q are continuous operators. Moreover, we obviously have the compatibility requirement that $E_Q E^-_\Omega w = 0$ whenever $\gamma_{\Omega\to\Sigma} w = 0$. The corresponding requirement for the case that $\gamma_{Q\to\Sigma} v = 0$ for $v \in H(Q)$ is slightly more complicated: In this case we necessarily have that $v|_\Sigma$ is constant over Σ, and hence, $\hat\gamma^-_{\Omega\to\Sigma} v|_\Sigma$ is a constant also. This shows that the restriction of $E^-_Q v$ to Ω is a constant function, and hence $E_\Omega E^-_Q v = 0$ by virtue of (4.2).

Finally, given

$$\psi \in H'(\Sigma) = \left\{ \psi \in H^{-1/2}(\Sigma) : \int_\Sigma \psi \,\mathrm{d}o = 0 \right\},$$

the variational problem

$$\int_Q \nabla v \cdot \nabla w \,\mathrm{d}x = \int_\Sigma \psi w \,\mathrm{d}o \qquad \text{for all } w \in H(Q) \tag{4.3}$$

has a unique solution $v \in H(Q)$, and this solution can be used to introduce the operator

$$L : H'(\Sigma) \to H(T), \qquad \psi \mapsto v|_T, \tag{4.4}$$

[1] When Ω consists of more than one connected component, the elements of $H(\Sigma)$ and $H(\Omega)$ need to have a vanishing mean over each connected component of Σ. The trace operator (4.1) then needs to be modified accordingly, i.e., by subtracting from v different constants on the different components of Σ. A similar comment applies to the restriction operator E_Ω of (4.2).

which will play a fundamental role in what follows. As in section 2, it can be shown that v is the physically relevant (weak) solution of the exterior Neumann problem

$$\Delta v = 0 \quad \text{in } Q, \qquad \frac{\partial v}{\partial \nu} = \psi \quad \text{on } \Sigma, \qquad \frac{\partial v}{\partial e_3} = 0 \quad \text{on } \mathbb{R}^2. \tag{4.5}$$

Now we can formulate our first main result, using the notation $\mathcal{R}(A)$ to denote the range space of some operator A.

THEOREM 4.1. *Under the assumptions* (1.2), (1.3), *there holds*

$$\mathcal{R}\big(|\Lambda_\sigma - \Lambda_{\mathbf{1}}|^{1/2}\big) = \mathcal{R}(L),$$

where L is given by (4.4).

Proof. The assertion is an immediate consequence of Theorem 3.1 in [12]. Except for the straightforward discussion of the bilinear forms occurring in [12], we have already verified all the assumptions of this theorem. Making use of the standard identification of $H'(\Sigma)$ with the dual space of $H(\Sigma)$, employing $L^2(\Sigma)$ as pivot space in the Gelfand triple, it is also obvious that the operator L of (4.4) is nothing but a reformulation of the operator L defined in [12]. ∎

We mention that the operator L of (4.4) and its dual operator appear naturally in a factorization of the difference of the two measurement operators,

$$\Lambda_\sigma - \Lambda_{\mathbf{1}} = LFL'$$

(cf. [12]), hence the name of the factorization method. Within the framework of Gebauer, an explicit derivation of this factorization and the operator F, in particular, is not necessary. In fact, a specification of F requires the introduction of some additional diffraction problems, similar to the ones in [6, 7]: Since we never need to return to this operator, we omit the details here, but rather refer the reader to [25] or the aforementioned papers for the details.

5. The range test. The range identity of Theorem 4.1 can be exploited to characterize the set Ω, since the range of L is easy to describe.

THEOREM 5.1. *Let $z \in \mathbb{R}^3_+$ be arbitrarily chosen. Then, for every $d \in \mathbb{R}^3 \setminus \{0\}$ the function*

$$g_{z,d}(x) = \frac{d \cdot (x - z)}{|x - z|^3}, \qquad x \in T, \tag{5.1}$$

belongs to $\mathcal{R}(L)$ if and only if $z \in \Omega$.

Proof. We first observe that $g_{z,d} = u_{z,d}|_T$, where

$$u_{z,d}(x) = \frac{1}{2}\, d \cdot \nabla_z \left(\frac{1}{|x - z|} + \frac{1}{|x - z'|} \right), \qquad x \in \mathbb{R}^3_+ \setminus \{z\},$$

is the superposition of two dipole potentials in z and z'. Here, $z' = z - 2(z \cdot e_3)e_3$ is the reflection of z with respect to the plane $\mathbb{R}^2$. Therefore, $u_{z,d}$ is a harmonic function in $\mathbb{R}^3_+ \setminus \{z\}$ with zero flux across $\mathbb{R}^2$. Moreover, $u_{z,d}$ belongs to $H(Q)$ if and only if $z \in \Omega$. Therefore, if $z \in \Omega$ and $\psi = \psi_{z,d}$ is the flux of $u_{z,d}$ across Σ into Ω, then $u_{z,d}$ is the solution of the exterior Neumann problem (4.5). Note that $\psi_{z,d}$ belongs to $H^{-1/2}(\Sigma)$; see, e.g., Girault and Raviart [13, Theorem 2.5]. Finally, we have for

$z \in \Omega$ that

$$\int_\Sigma \psi_{z,d}\,\mathrm{d}o_x = \frac{1}{2}\,d \cdot \nabla_z \left(\int_\Sigma \frac{\partial}{\partial \nu_x} \frac{1}{|x-z|}\,\mathrm{d}o_x + \int_\Sigma \frac{\partial}{\partial \nu_x} \frac{1}{|x-z'|}\,\mathrm{d}o_x \right) = \frac{1}{2}\,d \cdot \nabla_z \big(4\pi \mathbf{1}(z)\big) = 0$$

(see, e.g., [19, Example 6.16]), which shows that $\psi_{z,d} \in H'(\Sigma)$. We therefore have proved that $L\psi_{z,d} = g_{z,d}$, i.e., that $g_{z,d} \in \mathcal{R}(L)$ for $z \in \Omega$.

Now let $z \in \mathbb{R}^3_+ \setminus \Omega$, and assume that $g_{z,d} \in \mathcal{R}(L)$, i.e., that $g_{z,d} = L\psi$ for some $\psi \in H'(\Sigma)$. This is equivalent to the statement that $g_{z,d} = v|_T$, where $v \in H(Q)$ is the weak solution of (4.5). Thus, $u_{z,d}$ and v are two harmonic functions in $\mathbb{R}^3_+ \setminus (\{z\} \cup \overline{\Omega})$ which share the same Cauchy data on $\mathbb{R}^2$. By the uniqueness of the Cauchy problem (see, e.g., [9, Chapter II]) the two functions must be the same in $\mathbb{R}^3_+ \setminus (\{z\} \cup \overline{\Omega})$. This, however, contradicts the fact that $u_{z,d}$ has a singularity in z and, hence, does not belong to $H(Q)$. Therefore we have shown that $g_{z,d} \notin \mathcal{R}(L)$ whenever $z \in \mathbb{R}^3_+ \setminus \Omega$. ∎

As a corollary of Theorems 4.1 and 5.1 we obtain the following useful range test to decide whether some point $z \in \mathbb{R}^3_+$ belongs to Ω or not.

COROLLARY 5.2. *A point $z \in \mathbb{R}^3_+$ belongs to Ω if and only if the function $g_{z,d}$ of Theorem 5.1 belongs to the range of $|\Lambda_\sigma - \Lambda_{\mathbf{1}}|^{1/2}$.*

6. Numerical results. We now present a numerical realization of the range test of Corollary 5.2 for simulated data in three space dimensions. Data are given on $T = \Gamma = [0,2]^2$, shown as the somewhat darker area of the bounding plane in the subsequent figures. In all examples to follow, data have been generated by a boundary element method, with the conductivity within the inclusion being set to $\kappa = 0.5$. Modifications of κ have a negligible effect on the reconstructions, provided that (1.3) is satisfied for any small ε; this has been demonstrated convincingly in [7] for bounded domains in two space dimensions.

A very detailed discussion of the general approach for implementing the range test can be found in [7, 14], so here we focus mainly on the differences that are important for this half-space problem.

The first major difference is the fact that data are given on a two-dimensional interval rather than a one-dimensional interval. We have found it convenient to use tensor products of piecewise constant Haar wavelets (with vanishing mean over Γ) as current patterns and to expand the simulated potentials in the same orthogonal basis. The data we use thus correspond to the Galerkin projection of $\Lambda_\sigma - \Lambda_{\mathbf{1}}$ onto the space of the particular current patterns. All our computations use the corresponding first 1023 basis functions, which are far more than is required for the resolution of our reconstructions due to the inevitable presence of noise in the data.

Figure 6.1 reveals a second major difference from the results in [7, 14], which appears to be a characteristic property of the factorization method in three space dimensions. The eigenvalues of $\Lambda_\sigma - \Lambda_{\mathbf{1}}$ do not obey a strict geometric decay; rather, they tend to come in clusters of increasing size. Note that, in theory, the function $g_{z,d}$ belongs to the range of $|\Lambda_\sigma - \Lambda_{\mathbf{1}}|^{1/2}$ if and only if the corresponding Picard series

$$\sum_{j=1}^{\infty} \frac{\langle g_{z,d}, v_j \rangle^2_{L^2(\Gamma)}}{|\lambda_j|} \tag{6.1}$$

converges; here v_j, $j \in \mathbb{N}$, are the orthonormal eigenfunctions of $\Lambda_\sigma - \Lambda_{\mathbf{1}}$, and λ_j are the associated eigenvalues. In [7, 14] we have estimated the geometric decay of the

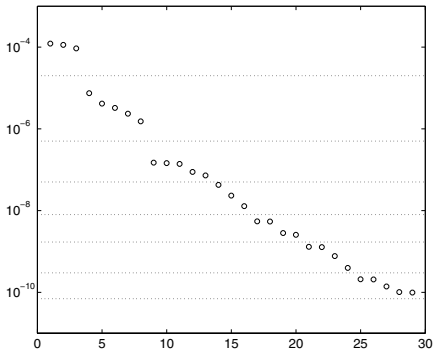

FIG. 6.1. *First test case: eigenvalues of* $\Lambda_\sigma - \Lambda_{\mathbf{1}}$.

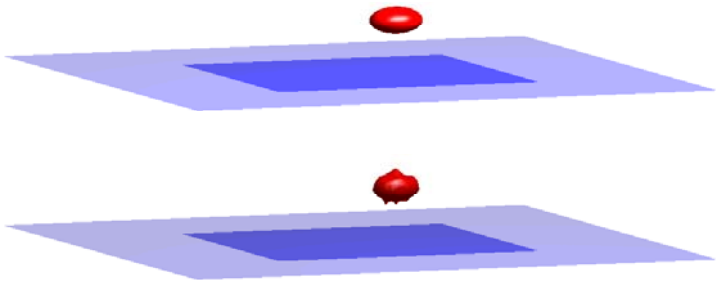

FIG. 6.2. *First test case: an ellipsoidal object (top) and its reconstruction (bottom).*

individual terms of this series to decide whether we believe that (6.1) converges or not. Here, instead, we have decided to average the eigenvalue clusters and investigate the root convergence factor of the geometric decay of the associated partial sums. The eigenvalue plot in Figure 6.1 (and similarly in Figure 6.4) contains dotted lines to indicate the eigenvalues that were considered to be clustered. The clustering has always been performed manually and is optimized to some extent to improve the quality of the reconstructions. Eigenvalue clusters below 10^{-10} have been ignored (except for section 6.4).

6.1. First test case. In the first example, which we have already mentioned, the object to be reconstructed is an ellipsoid with center in $P = (1.2, 0.8, 0.4)$ as shown in Figure 6.2. Its semiaxes are aligned with the coordinate axes and have radii $r_1 = 0.2$, $r_2 = 0.15$, and $r_3 = 0.1$. This isosurface plot is based on a certain average of the root convergence factors obtained from nine different dipole moments d_k, $k = 1, \ldots, 9$. (We refer the reader to [25] for further details.) We emphasize, as this might be difficult to see, that the reconstruction is at the correct place and has about the right size. It is only the boundary which is not accurate. Alternatively, we have also evaluated the series (6.1) for the respective range of eigenvalues and have used this function of z for a surface plot, as was done, e.g., by Kirsch in [18]. However, this gave somewhat inferior reconstructions.

6.2. Second test case. Our second example (see Figures 6.3 and 6.4) consists of two objects. One is an ellipsoid with center in $P = (0.4, 0.4, 0.4)$ and radii

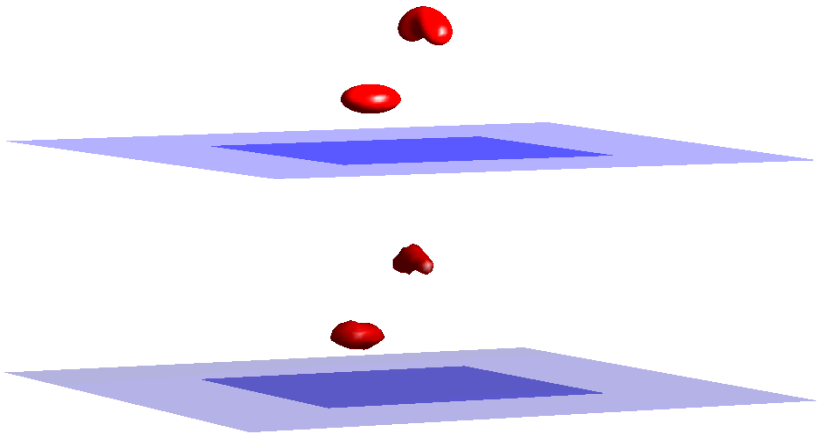

FIG. 6.3. *Second test case: two objects (top) and their reconstruction (bottom).*

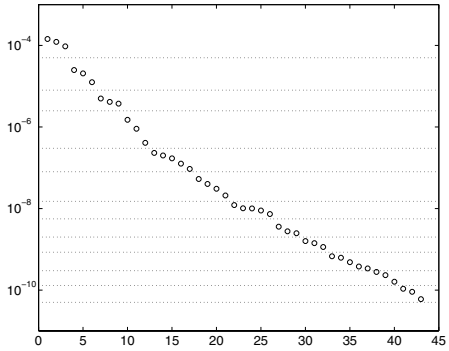

FIG. 6.4. *Eigenvalues for the second test case.*

$r_1 = r_2 = 0.2$ and $r_3 = 0.1$, respectively; again, the semiaxes are aligned with the coordinate axes. The other object has the shape of a kidney and is located around the point $Q = (1.2, 1.2, 0.8)$. The corresponding reconstructions are again at the correct locations. Note that the nonconvexity of the kidney is still well depicted, although it is a little farther away from Γ. On the other hand, its reconstruction is somewhat too small. If the nonconvex boundary is turned upwards, however, the reconstruction is qualitatively worse.

6.3. Third test case. The third test case is similar to the previous one, but now the ellipsoidal object is moved off to the side; i.e., its orthogonal projection onto $\mathbb{R}^2$ is outside of Γ; see Figure 6.5. More precisely, the ellipsoid of the second test case now has its center at $R = (-0.2, -0.2, 0.4)$. Our method reconstructs both objects at their true locations, but the reconstruction of the ellipsoid exhibits typical shady artifacts, similar to two-dimensional reconstructions shown in [14].

6.4. Fourth test case. For the next experiment we return to the ellipsoid from our first example, and increase its vertical distance to the plane. Figure 6.6 shows the reconstructions for three snapshots. As one expects, the quality deteriorates with

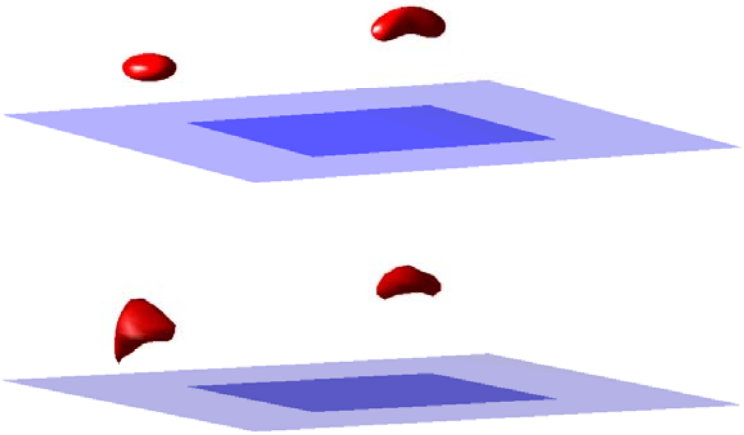

FIG. 6.5. *Third test case: two objects (top), one being off to the side, and their reconstruction (bottom).*

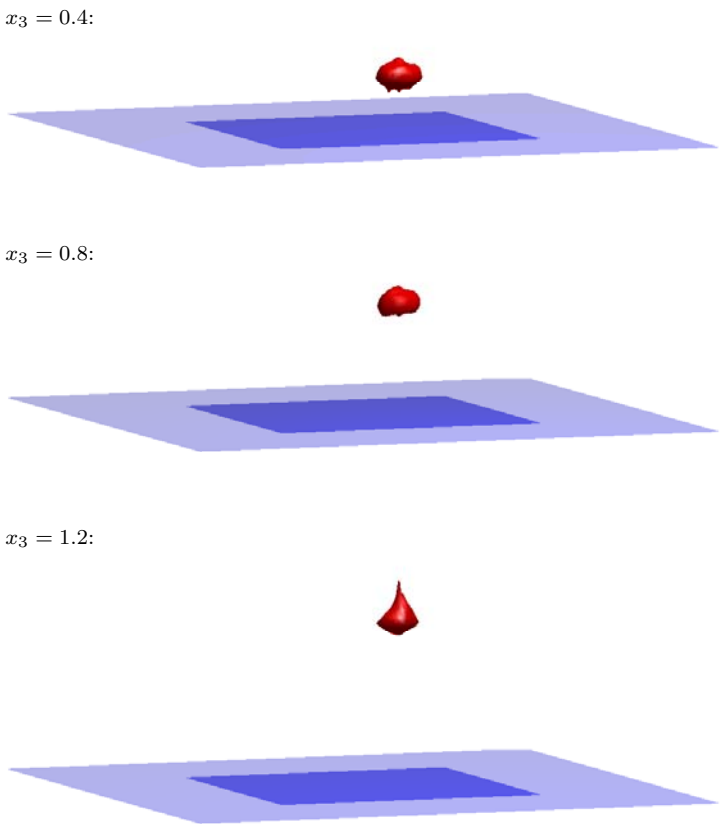

FIG. 6.6. *Fourth test case: reconstructions of ellipsoids with increasing vertical heights.*

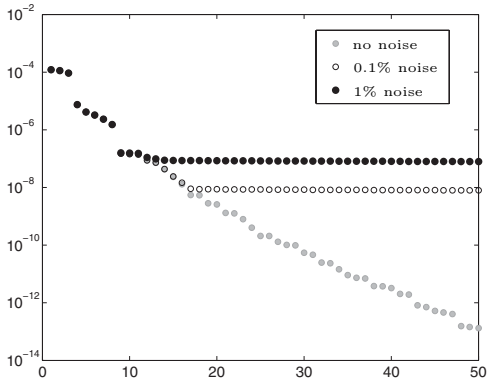

FIG. 6.7. *Eigenvalues in the presence of noise.*

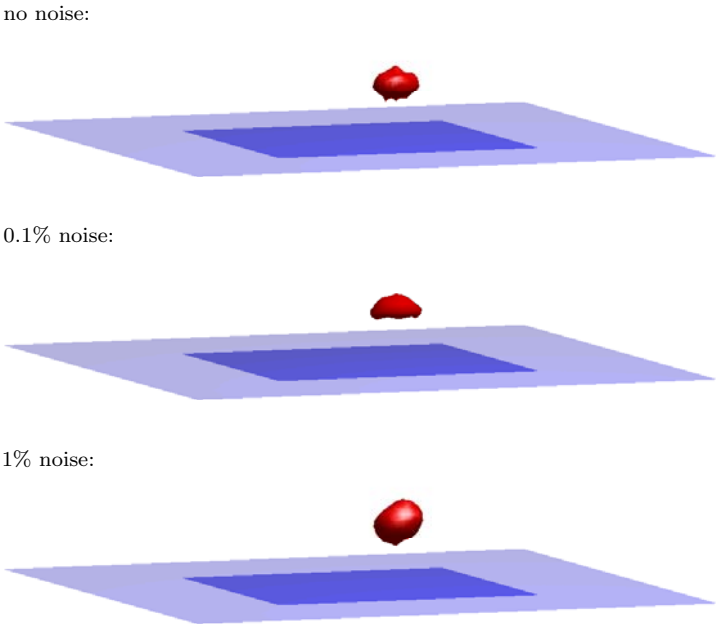

FIG. 6.8. *Reconstructions in the presence of noise.*

increasing distance x_3, measured at the center of the ellipsoid; see Figure 6.6. For these reconstructions we have used a slightly larger range of eigenvalues, going down to 10^{-12}.

6.5. Fifth test case. In a final study, we investigate the influence of noise on our reconstructions. To this end we superpose the data of our first test case (cf. Figure 6.2) with 0.1% and 1% noise, respectively. (These noise levels refer to the L^2-norms of the noise over the L^2-norm of the exact data.) Figure 6.7 shows the resulting eigenvalues of $\Lambda_\sigma - \Lambda_{\mathbf{1}}$. It is easy to see how the eigenvalues level off in the presence of noise, from which we can easily determine which eigenvalues can reliably be used to perform the range test. Figure 6.8 shows the corresponding reconstructions, which are quite reasonable even with 1% noise (bottom reconstruction).

7. The two-dimensional case. In this section we briefly comment on the modifications of our theory in two space dimensions; as a general reference we refer the reader to [25]. In two dimensions, solutions of the boundary value problem

$$\nabla \cdot \sigma \nabla u = 0 \quad \text{in } \mathbb{R}^2_+, \qquad -\sigma \frac{\partial u}{\partial e_2} = f \quad \text{on } \mathbb{R}, \tag{7.1}$$

are unique (up to additive constants) within the space $H^{1,0+}(\mathbb{R}^2_+)$ which is obtained by closing either $C^\infty(\mathbb{R}^2_+)$ or $C_0^\infty(\mathbb{R}^2_+)$ with respect to the inner product (2.6) for any $\alpha > 0$ (replacing the integrals by integrals over $\mathbb{R}^2_+$, of course). These spaces all contain the same functions, independent of the choice of $\alpha > 0$, including in particular the constant functions. We can get rid of these constants by turning to the quotient space $H(\mathbb{R}^2_+) = H^{1,0+}(\mathbb{R}^2_+)/\operatorname{span}\{\mathbf{1}\}$, for which we can use the H^1-seminorm as an equivalent norm.

Investigating the weak formulation of (7.1), the existence of a solution in $H^{1,0+}(\mathbb{R}^2_+)$ is guaranteed provided that the imposed current f belongs to

$$L^{2,-1-\alpha}_\diamond(\mathbb{R}) = \left\{ f : (1+|y|^2)^{1/2+\alpha/2} f \in L^2(\mathbb{R}) : \int_T f \, \mathrm{d}y = 0 \right\}$$

for some $\alpha > 0$; note that the normalization condition $\int_T f \, \mathrm{d}y = 0$ has not been required in the three-dimensional case.

Since the solution u of (7.1) is unique only up to additive constants, it is necessary to normalize the trace of u to set up a well-defined associated Neumann-to-Dirichlet operator. Accordingly, the general framework developed in section 4 requires some obvious changes for two space dimensions; in particular, a similar normalization is required in the definition of the operator L of (4.4). With these modifications, however, the result of Theorem 4.1 remains true, and a valid test function to be used in Theorem 5.1 (again, up to a suitable additive constant) is given by

$$g_{z,d}(x) = \frac{d \cdot (x-z)}{|x-z|^2}, \qquad x \in T. \tag{7.2}$$

We refer the reader to [25] for several numerical reconstructions in two space dimensions; preliminary results had been published in [14] and [24].

Appendix. In this appendix we prove that the weighted Sobolev space $H_{1/2+}(\mathbb{R}^3_+)$ introduced in Remark 2.3 is the direct sum

$$H_{1/2+}(\mathbb{R}^3_+) = H(\mathbb{R}^3_+) \oplus \operatorname{span}\{\mathbf{1}\}.$$

In the proof of this result we use the following Liouville-type theorem on bounded harmonic functions in the entire space, which appears to be of independent interest.

THEOREM A.1. *Every harmonic function u over $\mathbb{R}^3$ which satisfies*

$$\int_{\mathbb{R}^3} \frac{|u(x)|^2}{(1+|x|^2)^{5/2}} \, \mathrm{d}x < \infty \tag{A.1}$$

is a constant.

Proof. Our proof makes use of an appropriate modification of the argument given in Axler, Bourdon, and Ramey [1], which starts with the mean-value property of

harmonic functions, to write

$$|u(x^*) - u(0)| = \frac{3}{4\pi r^3} \left| \int_{B_r(x^*)} u(x)\,\mathrm{d}x - \int_{B_r(0)} u(x)\,\mathrm{d}x \right| = \frac{3}{4\pi r^3} \left| \int_{D_r} s(x)u(x)\,\mathrm{d}x \right|$$

for any fixed $x^* \in \mathbb{R}^3$. In this equation $B_r(y)$ denotes the ball of radius r around y, $D_r = B_r(x) \cup B_r(0) \setminus (B_r(x) \cap B_r(0))$ is the symmetric difference of the two balls, and s is a sign function that attains the two values ± 1 in the respective components of D_r. We denote $|x^*|$ by r^* and restrict r to be larger than $r_0 \geq 2r^* + 1$ in what follows. Then D_r is contained in the annulus

$$A_r = \{x \in \mathbb{R}^3 : r - r^* < |x| < r + r^*\},$$

and we can estimate

$$|u(x^*) - u(0)| \leq \frac{3}{4\pi r^3} \int_{A_r} |u(x)|\,\mathrm{d}x \leq c \int_{A_r} \frac{|u(x)|}{(1+|x|^2)^{3/2}}\,\mathrm{d}x,$$

where, from now on, we use c to denote a generic positive constant, depending only on x^*. Integrating the above inequality from $r = r_0$ to some $R > r_0$, we obtain

$$\begin{aligned} |u(x^*) - u(0)| &\leq \frac{c}{R - r_0} \int_{r_0}^{R} \int_{A_r} \frac{|u(x)|}{(1+|x|^2)^{3/2}}\,\mathrm{d}x\,\mathrm{d}r \\ &\leq \frac{2r^* c}{R - r_0} \int_{r_0 - r^* < |x| < R + r^*} \frac{|u(x)|}{(1+|x|^2)^{3/2}}\,\mathrm{d}x. \end{aligned}$$

Thus, the Cauchy–Schwarz inequality yields

$$\begin{aligned} |u(x^*) - u(0)|^2 &\leq \frac{c}{(R-r_0)^2} \int_{|x|>r_0-r^*} \frac{|u(x)|^2}{(1+|x|^2)^{5/2}}\,\mathrm{d}x \int_{|x|<R+r^*} \frac{1}{(1+|x|^2)^{1/2}}\,\mathrm{d}x \\ &\leq \frac{c}{(R-r_0)^2} \int_{|x|>r_0-r^*} \frac{|u(x)|^2}{(1+|x|^2)^{5/2}}\,\mathrm{d}x \int_0^{R+r^*} (1+r^2)^{1/2}\,\mathrm{d}r \\ &\leq c \left(\frac{R + r^* + 1}{R - r_0} \right)^2 \int_{|x|>r_0-r^*} \frac{|u(x)|^2}{(1+|x|^2)^{5/2}}\,\mathrm{d}x. \end{aligned}$$

Now, if R is sufficiently large, then we can choose $r_0 = R/2$ and thus obtain

$$|u(x^*) - u(0)|^2 \leq c \int_{|x|>R/2-r^*} \frac{|u(x)|^2}{(1+|x|^2)^{5/2}}\,\mathrm{d}x = o(1)$$

as $R \to \infty$. It follows that $u(x^*) = u(0)$, i.e., that u is a constant. ∎

We mention that this result is sharp in that all polynomials u in x of exact degree one are harmonic in $\mathbb{R}^3$ and satisfy (A.1) for any exponent in the denominator bigger than $5/2$.

Now we turn to verify (2.7). Let $w \in H_{1/2+}(\mathbb{R}^3_+)$, and consider the variational problem

$$\int_{\mathbb{R}^3_+} \nabla w_0(x) \cdot \nabla v(x)\,\mathrm{d}x = \int_{\mathbb{R}^3_+} \nabla w(x) \cdot \nabla v(x)\,\mathrm{d}x \qquad \text{for all } v \in H(\mathbb{R}^3_+).$$

This problem has a unique solution $w_0 \in H(\mathbb{R}^3_+)$, and it follows that $u = w - w_0 \in H_{1/2+}(\mathbb{R}^3_+)$ satisfies

$$\int_{\mathbb{R}^3_+} \nabla u(x) \cdot \nabla v(x)\, \mathrm{d}x = 0$$

for all $v \in C_0^\infty(\overline{\mathbb{R}^3_+})$, and hence, according to Weyl's lemma, u is a harmonic function in $\mathbb{R}^3_+$ with vanishing Neumann boundary values on the boundary of this half-space. Thus, u can be extended by reflection to an even harmonic function $\tilde{u}$ over the entire space $\mathbb{R}^3$; cf., e.g., [1]. As $u \in H_{1/2+}(\mathbb{R}^3_+)$ and hence has finite norm (2.6) for any $\alpha > 1/2$, it follows that $\tilde{u}$ satisfies (A.1). Thus $\tilde{u}$ and u are constant functions by virtue of Theorem A.1, and we have shown that any function $w \in H_{1/2+}(\mathbb{R}^3_+)$ can be decomposed in a unique way as $w = w_0 + c$, where $w_0 \in H(\mathbb{R}^3_+)$ and c is some constant. This proves (2.7).

REFERENCES

[1] S. Axler, P. Bourdon, and W. Ramey, *Harmonic Function Theory*, 2nd ed., Springer, New York, 2001.

[2] M. Azzouz, M. Hanke, C. Oesterlein, and K. Schilcher, *The factorization method for electrical impedance tomography data from a new planar device*, Int. J. Biomed. Imaging, 2007 (2007), Article ID 83016.

[3] T. Z. Boulmezaoud, *On the Laplace operator and on the vector potential problems in the half-space: An approach using weighted spaces*, Math. Methods Appl. Sci., 26 (2003), pp. 633–669.

[4] L. Borcea, *Electrical impedance tomography*, Inverse Problems, 18 (2002), pp. R99–R136.

[5] L. Borcea, *Addendum to "Electrical impedance tomography,"* Inverse Problems, 19 (2003), pp. 997–998.

[6] M. Brühl, *Explicit characterization of inclusions in electrical impedance tomography*, SIAM J. Math. Anal., 32 (2001), pp. 1327–1341.

[7] M. Brühl and M. Hanke, *Numerical implementation of two noniterative methods for locating inclusions by impedance tomography*, Inverse Problems, 16 (2000), pp. 1029–1042.

[8] A. P. Calderón, *On an inverse boundary value problem*, in Seminar on Numerical Analysis and Its Application to Continuum Physics, W. H. Meyer and M. A. Raupp, eds., Soc. Brasil Mat., Rio de Janeiro, 1980, pp. 65–73; reprinted in Comput. Appl. Math., 25 (2006), pp. 133–138.

[9] R. Dautray and J.-L. Lions, *Mathematical Analysis and Numerical Methods for Science and Technology. Volume* 1: *Physical Origins and Classical Methods*, Springer, New York, 2000.

[10] J. Deny and J.-L. Lions, *Les espaces du type de Beppo Levi*, Ann. Inst. Fourier (Grenoble), 5 (1954), pp. 305–370.

[11] V. Druskin, *On the uniqueness of inverse problems from incomplete boundary data*, SIAM J. Appl. Math., 58 (1998), pp. 1591–1603.

[12] B. Gebauer, *The factorization method for real elliptic problems*, Z. Anal. Anwend., 25 (2006), pp. 81–102.

[13] V. Girault and P.-A. Raviart, *Finite Element Methods for Navier-Stokes Equations*, Springer, Berlin, 1986.

[14] M. Hanke and M. Brühl, *Recent progress in electrical impedance tomography*, Inverse Problems, 19 (2003), pp. 65–90.

[15] B. Hanouzet, *Espaces de Sobolev avec poids—application au problème de Dirichlet dans un demi espace*, Rend. Sem. Mat. Univ. Padova, 46 (1971), pp. 227–272.

[16] T. A. Hope and S. Iles, *Technology review: The use of electrical impedance scanning in the detection of breast cancer*, Breast Cancer Res., 6 (2004), pp. 69–74.

[17] R. Janßen, *Elliptic problems on unbounded domains*, SIAM J. Math. Anal., 17 (1986), pp. 1370–1389.

[18] A. Kirsch, *Characterization of the shape of the scattering obstacle using the spectral data of the far field operator*, Inverse Problems, 14 (1998), pp. 1489–1512.

[19] R. Kress, *Linear Integral Equations*, 2nd ed., Springer, New York, 1999.

[20] M. Lukaschewitsch, *Inversion of Geoelectric Boundary Data, a Non-Linear Ill-Posed Problem*, Dissertation, Universität Potsdam, Potsdam, Germany, 1999.

[21] M. Lukaschewitsch, P. Maass, and M. Pidcock, *Tikhonov regularization for electrical impedance tomography on unbounded domains*, Inverse Problems, 19 (2003), pp. 585–610.
[22] J. L. Mueller, D. Isaacson, and J. C. Newell, *Reconstruction of conductivity changes due to ventilation and perfusion from EIT data collected on a rectangular electrode array*, Physiol. Meas., 22 (2001), pp. 97–106.
[23] M. Renardy and R. C. Rogers, *An Introduction to Partial Differential Equations*, Springer, New York, 1993.
[24] B. Schappel, *Electrical impedance tomography in the half space: Locating obstacles by electrostatic measurements on the boundary*, in Proceedings of the 3rd World Congress on Industrial Process Tomography, Banff, AB, Canada, VCIPT, 2003, pp. 788–793.
[25] B. Schappel, *Die Faktorisierungsmethode für die elektrische Impedanztomographie im Halbraum*, Dissertation, Johannes Gutenberg-Universität Mainz, Mainz, Germany, 2005; available online from http://nbn-resolving.de/urn/resolver.pl?urn=urn:nbn:de:hebis:77-7427.
[26] C. van Berkel and W. R. B. Lionheart, *Reconstruction of a grounded object in an electrostatic halfspace with an indicator function*, Inverse Probl. Sci. Eng., 15 (2007), pp. 585–600.